Chemical Papers (2022) 76:3661–3677
https://doi.org/10.1007/s11696-022-02120-4

ORIGINAL PAPER

Performance evaluation of electrocoagulation using aluminum, iron and copper electrodes for removal of xanthate

Mustafa Çırak[1]

Received: 18 November 2021 / Accepted: 31 January 2022 / Published online: 21 February 2022

Abstract

The mineral industry consumes a large amount of xanthate as collector, especially for the sulfide mineral's flotation. Nonetheless, the significant amount of xanthate also discharged from the processing plants, in proportion to the amount of used xanthate. In this work, the hazardous aqueous xanthate was aimed to be removed from water using electrocoagulation with three different electrodes: aluminum, iron and copper. Three separate experimental setups and designs were formed. The response surface methodology was implemented for the estimation of mathematical models for each electrode used in the electrocoagulation. All models were found statistically significant with p-values < 0.0015 and adjusted R^2-values > 0.95. According to the formed linear and quadratic models, the commonly used aluminum electrodes in the literature proved to be useless for the elimination of xanthate. The dissolved aluminum could not react with xanthate, and no precipitation was observed during the treatment. Iron electrode yielded better results than aluminum when the system parameters were statistically optimized at pH 6.54 and electrical current of 0.6 A. The most effective formation of hydroxyl ferric xanthates was actualized at these specific levels of parameters, and the maximum removal% of xanthate was obtained as 82.34%. On the other hand, the last electrode made from copper remarkably decreased the concentration of xanthate with a removal% of 100%. The copper ions released from the electrodes with the help of electricity had a great affinity for xanthate. Following the electrocoagulation process, Cu(I) ethyl xanthate/Cu(II) ethyl xanthate efficiently precipitated, forming a yellow solid sediment at the bottom of the reactor. Consequently, the maximum desirability values for the removal of xanthate were found as 0.0037, 0.7700 and 1.000 respectively for aluminum, iron and copper electrodes. Based on this statistical optimization, the copper electrodes enabled the accomplished separation of hazardous xanthate from water using electrocoagulation at pH 9 and electrical current of 0.6 A.

Keywords Xanthate · Electrocoagulation · Electrode · RSM · Optimization

Introduction

The mineral industry, all around the world, employs a physicochemical technique called froth flotation, especially for the concentration of sulfide-containing complex ore deposits. This flotation method is a three-phase system comprising solid minerals, liquid water molecules and air bubbles. It relies on the differences between the surfaces of the natural mineral particles (Harjanto et al. 2021). The principle idea behind this physicochemical separation is to render the desired (valuable) mineral's surface hydrophobic and the undesired particles hydrophilic. Once this surface rendering process is completed, the hydrophobic (air-avid) particles are attached themselves to air bubbles and rise upward altogether by under SG_{air} bubbles $< SG_{water}$. On the other hand, the hydrophilic (water-avid) particles prefer to contact water molecules instead of air bubbles (Farrokhpay 2011). The concentration is effectuated by simply removing of top froth layer that involves valuable hydrophobic particles.

The flotation reagents, which make a mineral's surface hydrophobic, are called as collector. There are varying types of collectors that are specifically designed depending on the physical and chemical properties of the targeted minerals. Xanthate is the most common collector for the flotation of complex sulfide ores (Chen et al. 2021). This reagent is categorized as an anionic collector with a combination of carbon dioxide, sodium hydroxide and alcohol. It presents a mild

✉ Mustafa Çırak
mustafa.cirak@gmail.com

[1] Mining Engineering Department, Muğla Sıtkı Koçman University (MSKU), Muğla, Turkey

acid property in an aqueous medium. The number of carbon in its molecular structure determines its collecting power in the flotation process (Kang and Hu 2017). Xanthates with a carbon number of 2 or less provide a weak floatability to the sulfide ores, and they are only applicable to easily floatable minerals. However, xanthates with a larger number of carbon lead to a longer hydrocarbon chain in their molecular structure. Once these longer hydrocarbon chains adsorb on the mineral surface, forming head-to-tail extension into the water, the solid matter becomes more hydrophobic. It also results in higher recoveries considering the process efficiencies (Chen et al. 2021).

Xanthate can be used for several mineral flotation plants industrially. For example, pyrite concentration can be done by the xanthate application at slightly acidic pH values (Mu et al. 2015). Galena processing plants also benefit from the xanthate collecting ability at a pH of 7–9 (Vučinić et al. 2006). Many other sulfide minerals that contain copper and sulfur can be enriched easily since there is a high affinity between Cu^{++} on the surface and xanthate molecules (Bowden and Young 2016). Although sphalerite has a low floatability, xanthate can be used to make this mineral hydrophobic provided that its surface is initially activated with Cu^{++} ions. As it can be understood from these mineral industries that compulsorily rely on the vast amount of the collector consumption, there is an overgrowing worldwide demand for xanthate as well as copper, lead, zinc, etc. Shen et al. (2020) estimated that the global annual xanthates consumption, just by the mining companies, will be over 370,000 tons in 2025.

The continuous increase in xanthate consumption may lead to detrimental occupational health and safety risks, environmental hazards and non-sustainable production (Shen et al. 2016). When xanthates are discharged from a processing plant or leaked from tailing ponds, they can easily mix with the underground water reservoir, natural spring waters or riverine/lake ecosystems. The presence of xanthates in such water bodies results in severe contamination. Xu et al. (1988) studied and proved the bioaccumulation of xanthate in aquatic organisms. For example, the plant called Lemna Minor can absorb xanthate with a bioaccumulation factor as high as 1000 (Xu et al. 1988). The cellular uptake of heavy metals like cadmium, lead copper also increased in direct proportion to the bioaccumulation of xanthate. This co-tendency was explained by the high chemical affinity between the heavy metals and xanthates. As a result, the contamination of xanthate becomes more hazardous since it carries strong complexes of heavy metals with it (Boening 1998).

Furthermore, the toxic effect of xanthate on aquatic organisms was studied in the literature. Bertillas et al. (1985) proved that the presence of xanthates in water bodies was severely toxic to fish, algae and bacteria. Nevertheless, it was observed (Bertillas et al. 1985) that there is an excellent increase in metal toxicity in the presence of heavy metals and xanthates /up to 3.5 times for fish 25 times for algae). In addition to its indirect metal toxication effect, xanthates can be hydrolyzed in the human body, degrading into alcohol and carbon disulfide. In particular, the latter degradation product can cause acute toxicity with several health issues like reproductive effect and neurological problems DeMartino et al. 2017). The handling, transportation and application of xanthate should be carried out very carefully because the previously mentioned carbon disulfide can be released with an intensive decomposition of xanthate in an alkali media. This undesirable decomposition during the process can affect sustainable production (loss of reagent), and it releases very toxic (and flammable) gas in the working area.

In this work, an alternative electricity-based treatment, which has not been previously practiced in the published literature to eliminate xanthate contamination in water, was experimented. The primary objective (1) was to investigate the applicability of the electrocoagulation process for the treatment of xanthate-containing water. Secondly (2), three different metal electrodes were attached to the electrocoagulation reactor to reveal the metal-dependent performance of the process, comparatively. Thirdly (3), the statistical models were estimated using response surface methodology based on the experimental data. Thereafter (4), the effect of the parameters (pH and electrical current) on the treatment efficacy was explained one by one for each electrode type. Finally (5), the optimization study was conducted to determine the best-operating conditions and metal type for this physicochemical process.

Material and methods

Xanthate, which is a typical collector used for the flotation of complex sulfide ores in the mineral industry (Ackerman et al. 1987), was procured from a local supplier (ECS Kimya). However, in this work, xanthate was preferred to mimic a specific aqueous contaminant generated in mineral processing plants. The required amount of xanthate pellets were mixed and wholly dissolved in 1 L of distilled water (TDS < 1 ppm) at 1000 rpm. The resultant stock solution had a concentration of 2 mM.

SOIF UV-5100H Single Beam Spectrophotometer (UV/VIS 200–1000 nm) was used to determine xanthate concentration. The xanthate-containing solution was firstly analyzed between 250 and 340 nm. The output spectrum between these wavenumbers was stated, and a unique peak was identified at 301 nm. The previous research papers (Prestidge et al. 1994; Fornasiero et al. 1995; Grano et al. 1997; Sun and Forsling 1997; Hao et al. 2008; Agorhom et al. 2014) also confirm this same peak value of xanthate.

The spectrophotometric analysis to determine xanthate concentration was conducted at 301 nm. In the next stage, varying concentrations from the pure water to the xanthate-containing stock solution were tested, and the corresponding absorbance values were plotted. A linear model was obtained after a statistical regression between the collected data points with a large R^2-value of 0.9956. This model identified the variation in the data with the following equation: $y = 0.0888x + 0.0037$. Based on this linear equation between the absorbance and the concentration, all required concentrations were estimated, contributing to the performance evaluation of the electrocoagulation experiments.

Three different sets of experiments were carried out considering the previously mentioned setups in published literature (Akansha et al. 2020; Balouchi et al. 2020). The chemical compositions of the aluminum, iron and copper electrodes were 99.95%-Al, 98.6%-Fe and 99.5%-Cu. Aluminum, iron and copper electrodes were separately tested to remove the aqueous xanthate. These experimental setups are shown in Fig. 1. 150 mL representative samples was taken from the xanthate-containing stock solution. Then, they were put into 200-ml beakers for each experiment and vigorously mixed with the help of the magnetic stirrer beneath the beaker. Following that, the desired metal electrode was dipped into this solution. The electrodes were wired to GWINSTEK Power Supply for the completion of the circuit of the electrocoagulation reactor.

The two most critical independent parameters were selected and used during the electrocoagulation experiments: the pH of the solution (X_1) and the applied electrical current (X_2). The desired value of the solution pH was adjusted by using 0.1 M NaOH or 0.1 M HCl. The minimum (− 1), intermediate (0) and maximum (1) values of the solution pH were 5, 7 and 9, respectively. The desired values of the applied electrical current were adjusted by using a digital panel of the power supply. The minimum (− 1), intermediate (0) and maximum (1) values of the applied electrical current were 0.1 A, 0.35 A and 0.6 A, respectively. The experimental design + response surface methodology had been implemented to statistically analyze the effect of these parameters on the xanthate removal % (Y). The face-centered central composite design method, as one of the most commonly preferred fractional factorial designs in the literature (Bhattacharya 2021), was used for the systematic investigation of these process parameters, especially in the water treatment discipline (Karimifard and Moghaddam 2018; Nasseri et al. 2020; Saber et al. 2021). For the statistical evaluation and modeling of the obtained experimental data, Design Expert (Demo Ver.) software was used. The software generated a certain number of random runs for the central

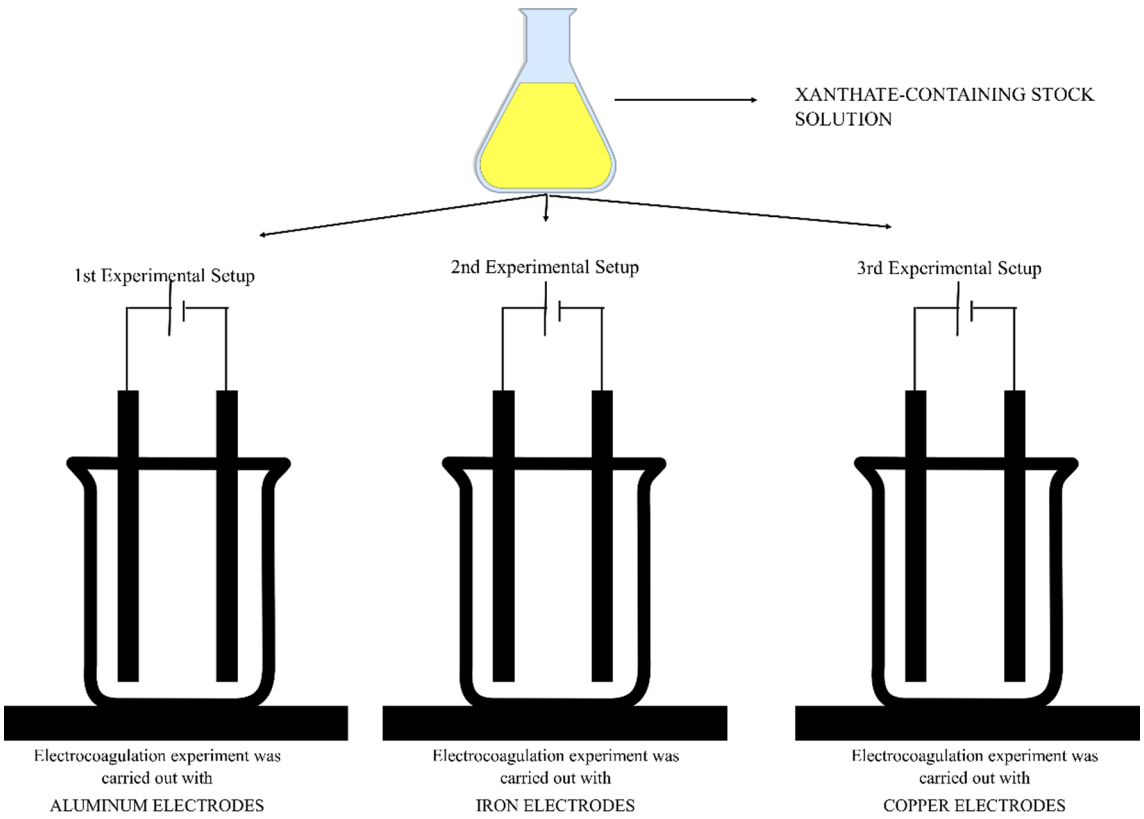

Fig. 1 Experimental setup of electrocoagulation

composite design, and the related experimental template was determined as stated in Table 1. Once all required experimental results were completed in the laboratory, the xanthate removal % was introduced to the software as the response values (Table 1):

1. The best models for each experimental setup were designated regarding the statistical indicators.
2. The response surfaces were formed within the experimental boundaries.
3. The parameters were optimized for the maximum removal percentages of xanthate.

With the help of this statistical work, the effect of the parameters on the responses, the proper electrode selection, the highest performance achievements for each electrode (aluminum, iron or copper) was aimed to be revealed for the treatment of this harmful chemical used frequently in the mining industry.

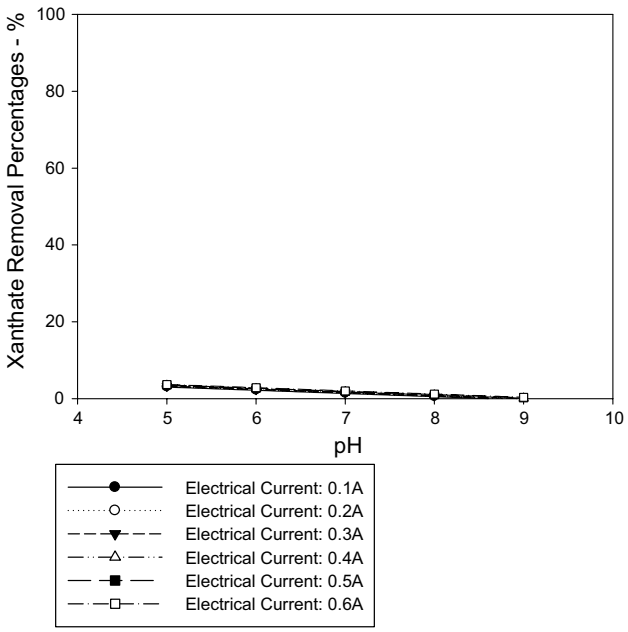

Fig. 2 Electrocoagulation by using aluminum electrodes

Results and discussion

Three electrocoagulation experiments were carried out with three different electrodes, aluminum, iron, copper. The mechanism of the process was tried to be explained with previously published adsorption/surface precipitation works since there is no current direct study related to the xanthate electrocoagulation in the literature.

Firstly, the aluminum electrodes were tested since this material was frequently used in wastewater treatments (Sharma et al. 2021; Sürme and Demirci 2014; Nyangi 2021). Figure 2 shows that the maximum removal efficiency of xanthate was only 4% in this case of electrocoagulation. Almost no chemical affinity was observed between aluminum released from the electrode and the aqueous xanthate. The color of the solution could not be cleared. The worst electrocoagulation performance was obtained with aluminum within the studied range of the parameters. Although the literature (Rezaei et al. 2018; Amrollahi et al. 2019; Salarirada et al. 2021) indicated that the removal of xanthate is possible through its adsorption on the aluminum-activated solid surfaces like Al–bentonite, Al–activated carbon, etc., this experimental work showed that the direct precipitation with aluminum-based electrocoagulation was not possible. Iron was used as a second electrode material (Fig. 3). While the removal performance of the iron-based electrocoagulation was insufficiently low at pH 9, it became much better with a level of 80% at pH 6.5 comparing to the aluminum electrode. Noirant et al. (2019) claimed that the

Table 1 Face-centered central composite experimental design

Run#	pH of solution	Electrical current (A)	Experimental xanthate removal% with aluminum electrode	Experimental xanthate removal% with iron electrode	Experimental xanthate removal% with copper electrode
1	1	1	0	42	100
2	1	−1	0	25	59
3	−1	−1	3	45	45
4	0	−1	1	64	53
5	0	1	2	78	88
6	1	0	0	38	86
7	−1	0	3	62	63
8	−1	1	4	68	72
9	0	0	2	74	80

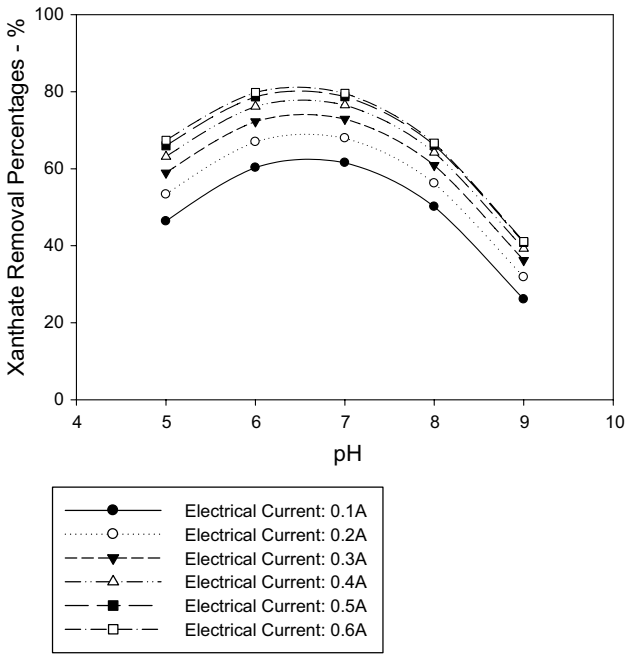

Fig. 3 Electrocoagulation by using iron electrodes

xanthate chemisorption is possible through iron on mineral surfaces. Deng et al. (2021) confirmed this and reported that iron xanthate can be formed on the pyrite surface. Another study (Amin et al. 2019) tested and proved that xanthate with aqueous iron in the absence of electricity was possible. The chemical affinity between the iron released from the electrodes and xanthate was affirmed with the literature, also. The copper electrode was tested as a third and final treatment. At pH 9, the copper-based electrocoagulation produced a proficient outcome of 100% removal of xanthate. The electrical current at 0.6 A also contributed to the success of the process. In the other physicochemical process like froth flotation, the dissolved copper can be used as an activator for sulfide minerals (Bu et al. 2019). Once the mineral surface was activated, the adsorption of xanthate can be enabled (Wang et al. 2019). This means that the xanthate chemisorbed itself on the particle through this copper (Xia et al. 2019). The copper ions have a strong complexation ability with xanthate as proved in this work. As a result, a superior removal of xanthate can be achieved with only copper electrodes rather than aluminum and iron.

After the completing of the laboratory tests, three collected data sets were statistically analyzed, and the different regression models were tested. The linear, 2FI, quadratic and cubic models' suitability was checked for each data set based on the p-value and R^2 as shown in Table 2. The first regression model that belongs to the electrocoagulation via aluminum electrodes were merely linear (p-value < 0.0001 and $R^2 = 0.9506$). On the other hand, the second (p-value < 0.0011 and $R^2 = 0.9858$) and third models (p-value < 0.0202 and $R^2 = 0.9911$) that represent the electrocoagulation via iron and copper electrodes were suggested in quadratic form. The minimal coefficients of the estimates of the linear model refer that pH levels (X_1) and electrical current (X_2) had almost no mathematical contribution on xanthate removal % (Y) throughout the electrocoagulation process when aluminum electrodes were used. Nonetheless,

Table 2 Comparison of the linear, 2FI, quadratic and cubic models

Model-1: Aluminum electrodes	Sequential	Adjusted	Predicted	
Source	p-value	R^2	R^2	
Linear	< 0.0001	0.9506	0.9085	Suggested
2FI	0.1438	0.9630	0.9189	
Quadratic	1.0000			
Cubic	0.7746	0.8889	− 1.5312	Aliased
Model-2: Iron electrodes	Sequential	Adjusted	Predicted	
Source	p-value	R^2	R^2	
Linear	0.1310	0.3229	− 0.0967	
2FI	0.8616	0.1929	− 1.2515	
Quadratic	0.0011	0.9858	0.9382	Suggested
Cubic	0.3549	0.9946	0.8776	Aliased
Model-3: Copper electrodes	Sequential	Adjusted	Predicted	
Source	p-value	R^2	R^2	
Linear	0.0003	0.9155	0.8549	
2FI	0.2095	0.9283	0.8261	
Quadratic	0.0202	0.9911	0.9723	Suggested
Cubic	0.9001	0.9784	0.5090	Aliased

Table 3 ANOVA tables and omission of nonsignificant terms

Initial version of Model-1 for aluminum electrodes							Improved version of Model-1 for aluminum electrodes (after statistically nonsignificant terms are removed)	Omitted terms
Source	Sum of squares	*df*	Mean square	*F* value	*p*-value Prob > *F*			
Model	17.33	2	8.67	78.00	< 0.0001	Significant	No terms required omission since all terms had a *P*-value < 0.05	No terms were omitted
A-A	16.67	1	16.67	150.00	< 0.0001	Significant		
B-B	0.67	1	0.67	6.00	0.0498	Significant		
Residual	0.67	6	0.11					
Cor total	18.00	8						
R^2	0.9630							
Adj R^2	0.9506							
Pred R^2	0.9085							
Adeq precision	20.785							

Initial version of Model-2 for iron electrodes							Improved version of Model-2 for iron electrodes (after statistically nonsignificant terms are removed)						Omitted terms
Source	Sum of squares	*df*	Mean square	*F* value	*p*-value Prob > *F*		Source	Sum of squares	*df*	Mean square	*F* value	*p*-value Prob > *F*	
Model	2632.78	5	526.56	111.94	0.0013	Significant	Model	2586.22	3	862.07	71.05	0.0002	Significant	AB B^2
A-A	1118.81	1	1118.81	237.86	0.0006	Significant	A-A	1112.65	1	1112.65	91.70	0.0002	Significant	
B-B	97.37	1	97.37	20.70	0.0199	Significant	B-B	486.00	1	486.00	40.05	0.0015	Significant	
AB	9.00	1	9.00	1.91	0.2606		A^2	1283.56	1	1283.56	105.79	0.0001	Significant	
A^2	1283.56	1	1283.56	272.88	0.0005	Significant	Residual	60.67	5	12.13				
B^2	37.56	1	37.56	7.98	0.0664		Cor total	2646.89	8					
Residual	14.11	3	4.70				R^2	0.9771						
Cor total	2646.89	8					Adj R^2	0.9633						
R^2	0.9947						Pred R^2	0.9258						
Adj R^2	0.9858						Adeq precision	23.684						
Pred R^2	0.9382													
Adeq precision	30.212													

Initial version of Model-3 for copper electrodes							Improved version of Model-3 for copper electrodes (after statistically nonsignificant terms are removed)						Omitted terms
Source	Sum of squares	*df*	Mean square	*F* value	*p*-value Prob > *F*		Source	Sum of squares	*df*	Mean square	*F* value	*p*-value Prob > *F*	
Model	2630.78	5	526.16	179.83	0.0006	Significant	Model	2614.72	4	653.68	105.29	0.0003	Significant	A^2
A-A	26.39	1	26.39	9.02	0.0575	–	A-A	53.61	1	53.61	8.64	0.0424	Significant	
B-B	80.90	1	80.90	27.65	0.0134	Significant	B-B	80.90	1	80.90	13.03	0.0226	Significant	
AB	49.00	1	49.00	16.75	0.0264	Significant	AB	49.00	1	49.00	7.89	0.0483	Significant	

Table 3 (continued)

Initial version of Model-3 for copper electrodes							Improved version of Model-3 for copper electrodes (after statistically nonsignificant terms are removed)						Omitted terms
Source	Sum of squares	*df*	Mean square	*F* value	*p*-value Prob > *F*		Source	Sum of squares	*df*	Mean square	*F* value	*p*-value Prob > *F*	
A^2	16.06	1	16.06	5.49	0.1010		B^2	93.39	1	93.39	15.04	0.0179	Significant
B^2	93.39	1	93.39	31.92	0.0110	Significant	Residual	24.83	4	6.21			
Residual	8.78	3	2.93				Cor total	2639.56	8				
Cor total	2639.56	8					R^2	0.9906					
R^2	0.9967						Adj R^2	0.9812					
Adj R^2	0.9911						Pred R^2	0.9657					
Pred R^2	0.9723						Adeq precision	30.153					
Adeq precision	40.096												

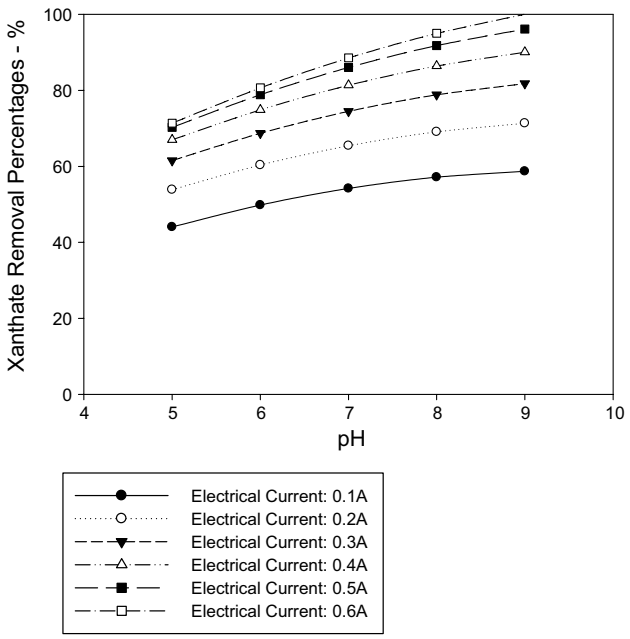

Fig. 4 Electrocoagulation by using copper electrodes

the coefficients of the estimates in Model-2 and Model-3 were higher, proving that the selected independent variables (X_1 and X_2) had a substantive practical effect on the response (Y) in the presence of iron and copper electrodes.

The suggested linear and quadratic models in Table 2 was investigated in detail and it was observed that some terms were statistically nonsignificant. These terms with a p-value > 0.05 were discarded from the initial models in Table 3, aiming for a higher capability for the modeling and optimization work. All terms in the initial Model-1 had a p-value < 0.05 and no improvement was required for this simple linear model. Also, the p-value of Model-1 more minor than 0.0001 confirmed the statistical significance of the estimated model. For Model-2, AB and B^2 in Model-2 and A^2 in Model-3 were omitted since they had a p-value of 0.2606, 0.0664 and 0.1010, respectively. All remaining terms had a statistical significance for this study, and they were included in the mathematical models.

ANOVA tables of the improved models indicated that the mathematical expressions are statistically significant since their p-values were smaller than 0.05, as shown in Table 3. This statement confirms that the models were capable of the proper representation of three experimental data sets. According to these models' R^2, adjusted-R^2 and predictive-R^2 values, the substantial amount of the total variation in the collected data sets was efficiently explained. For instance, all R^2-indicators were very close to the ideal/perfect case expounded by $R^2 = 1$. Adeq Precisions were also tested, and the resultant ratios showed a little noise and a high level of signal for each one. Therefore, adequate precision (20.785, 23.684 and 30.153, respectively) was proved for the estimated models since they were higher than the reference value 4.

The normal plots of the residuals were used as diagnostic tests to analyze the models graphically. As shown in Fig. 4, the residuals mostly intensified close to the red-colored straight lines, and there were no outlier data points throughout the plots. Since there was no non-normal error distribution, the normality assumptions were checked as valid. The proven normality and homoscedasticity (Fig. 5) provided an excellent ability to correctly forecast the xanthate removal

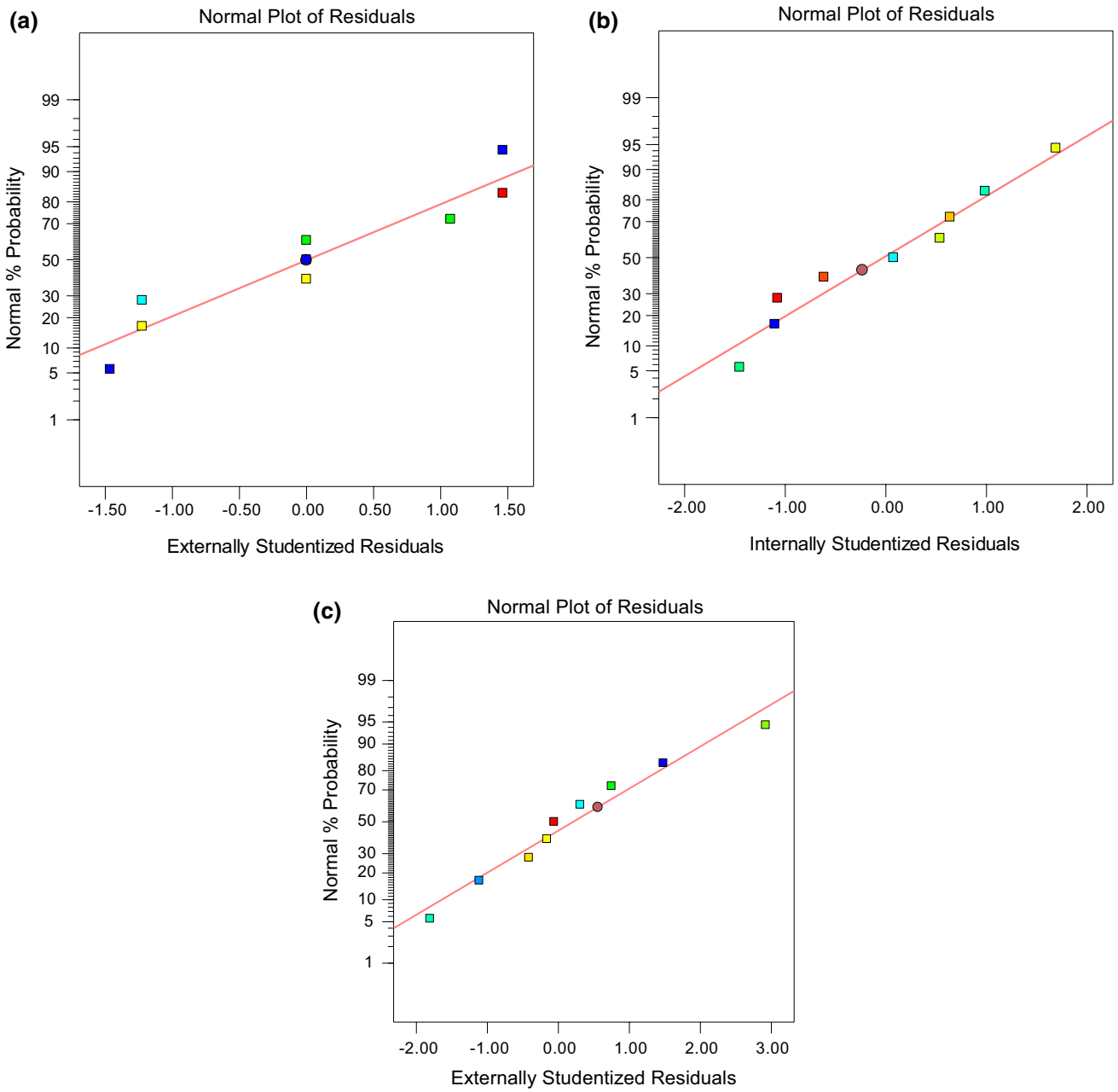

Fig. 5 Studentized residuals of the models (**a** Model-1, **b** Model-2, **c** Model-3)

percentages. The comparative plots of the observed versus the estimated response values (Fig. 6) showed that all data points followed a 45° angle line. This tendency endorsed the successful model fittings and the high level of prediction power of the linear and quadratic models.

The most common electrodes used in previously published electrocoagulation studies (Aitbara et al. 2016; Safwat et al. 2019; Zini et al. 2020) are aluminum electrodes. The solid aluminum electrodes dissolved and hydrolyzed into varying aqueous species under electrical current during the electrocoagulation process. The hydrolysis products of aluminum have been found very efficient for wastewater treatment. They form polynuclear species (Bertsch and Parker 1996) like $Al_2(OH)_2^{4+}$, $Al_2(OH)_5^{+}$, $Al_3(OH)_4^{5+}$, $Al_8(OH)_{20}(H_2O)_5^{4+}$, $Al_6(OH)_{12}(H_2O)_{12}^{6+}$, $Al_{54}(OH)_{144}(H_2O)_{36}^{18+}$ and $Al_{13}O_4(OH)_{24}(H_2O)_{12}^{7+}$ and these active aqueous phases can chemically interact and eliminate target matters in most wastewater, efficiently (Hu et al. 2016; Palacios et al. 2016). Based on this fact, the aluminum electrodes were tested for the removal of xanthate, and their results were stated in Fig. 7. The percentages of the xanthate removal were almost zero at pH

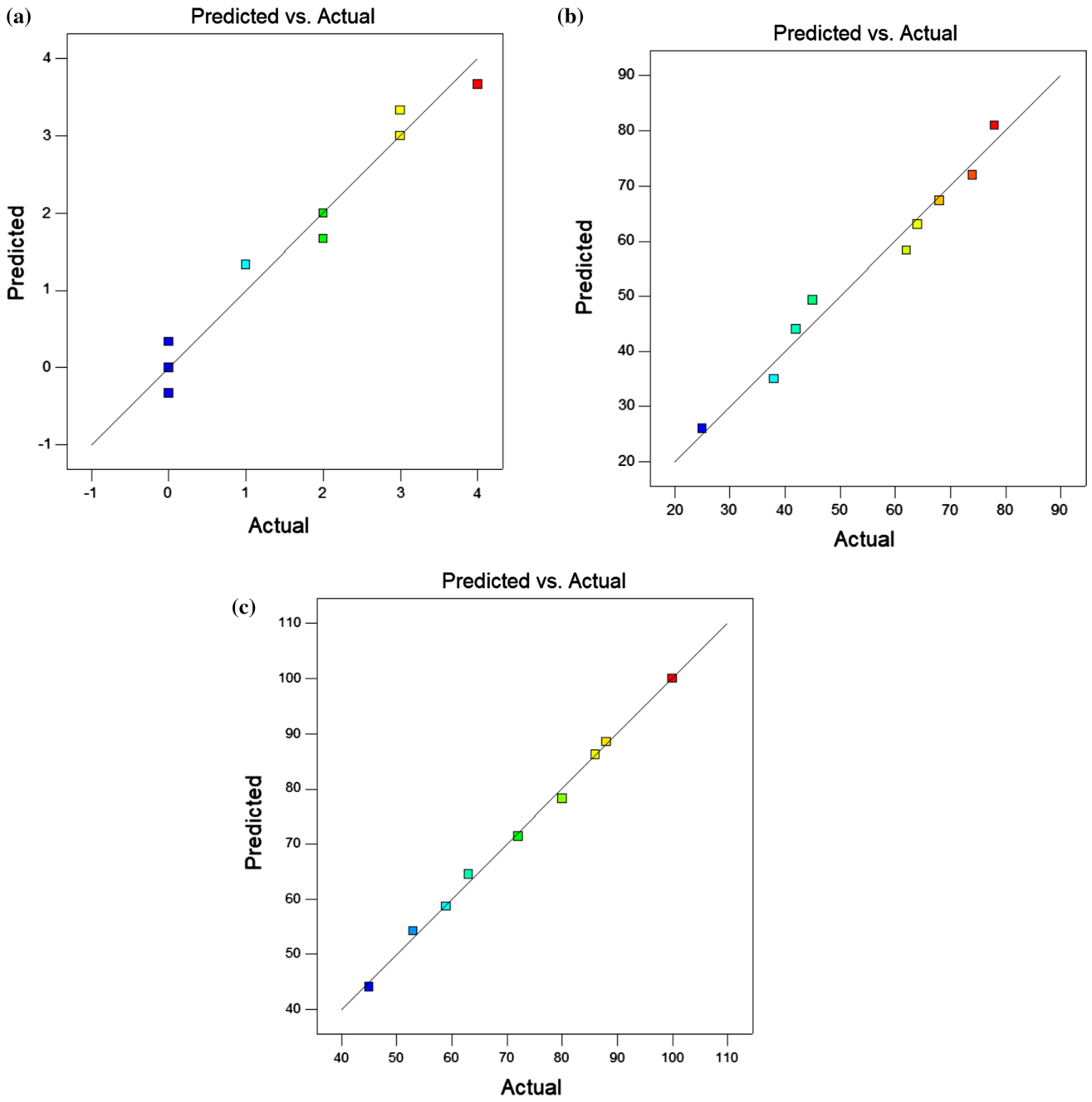

Fig. 6 Predicted versus actual (experimental) values (**a** Model-1, **b** Model-2, **c** Model-3)

9, and the increase in the electrical current by no means improved it. While pH reduced from 9 down to 5, a very slight variation was observed, xanthate removal efficiency was only around 3%, and the yellow-colored water contaminated by xanthate could not be treated with the aluminum electrodes. Although the dissolved aluminum forms potent coagulating agents, as mentioned above, they could not form insoluble compounds with xanthates. Conclusively, the expected sequence of the precipitation and coagulation failed throughout the studied range of the parameters.

Secondly, iron electrodes were attached to the electrocoagulation reactor, and the test results were summarized in the contour plots. The better xanthate removal efficiencies were obtained by using iron electrodes compared to the former aluminum electrodes. According to the generated lines in Fig. 7, the removal efficiencies were only between 24 and 42% at pH 9. The dissolved iron from the anode could not ably react with xanthate at this pH level. Iron ions principally precipitate as xanthate-free oxide forms (Sheikh and Leja 1977). When the solution pH was

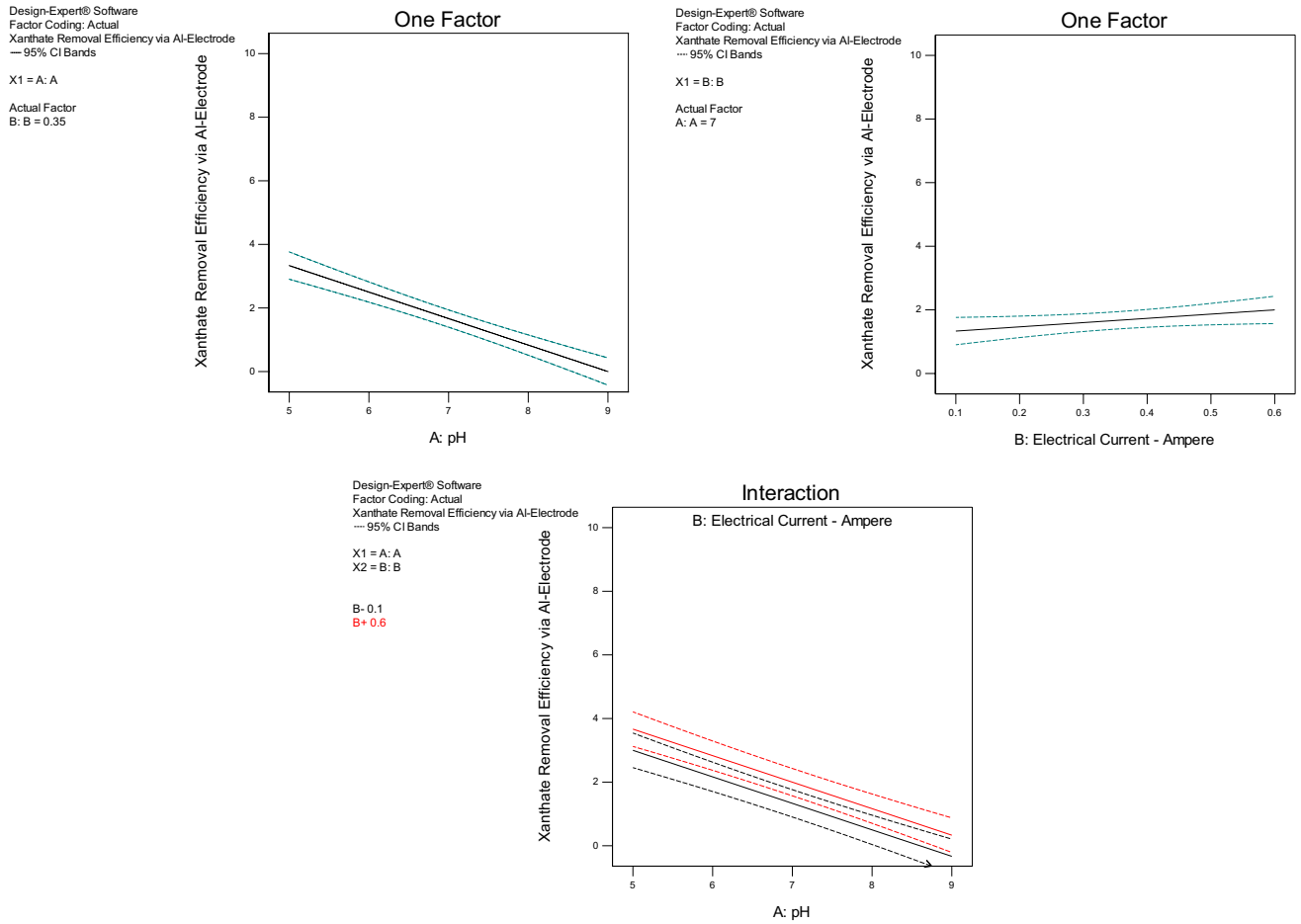

Fig. 7 Effect of individual factors and their synergistic interaction effect on xanthate removal when aluminum electrodes were implemented (Model-1)

adjusted to 6 and 7, a more efficient xanthate removal was observed since the co-precipitation of iron and xanthate took place instead of iron oxide phases. Nonetheless, Fig. 8 shows that the electrical current was significant, as much as the solution pH. The increase in the electrical current to 0.6 A at pH 6.5 expressively enhanced the efficiency of the process up to 82%. The previous researchers carried out the thermodynamic calculations about a similar system containing iron xanthate–water (Sheikh 1972). They found out that ferric xanthate $Fe(EX)_{3(solid)}$ can be observed regardless of whether Fe^{2+}, Fe^{3+}, EX^{-} and $(EX)_2$ are used as reactants under the relevant conditions, and it was clear that ferric xanthates are only stable in severe acidic conditions (Wang et al. 1989). On the other hand, hydroxyl ferric xanthates $Fe(OH)_n(EX)_{3\text{-}n(solid)}$ is precipitated since they are more stable around the neutral pH levels (Sheikh and Leja 1977). Based on this, the red-colored region on Figs. 8 and 10, which was obtained by using the iron electrodes at around $I = 0.6$ A and pH 6.5, thermodynamically corresponded to the precipitation zone of hydroxyl ferric xanthates. As a result, a more considerable amount of xanthates could be removed from water via iron electrodes due to the formation of the stable hydroxyl ferric xanthates, for instance, $Fe(OH)_2(EX)_{(solid)}$.

Thirdly, the copper electrodes were also tested to treat of the xanthate-contaminated water. However, the previously mentioned aluminum and iron electrodes have been more commonly used in the related literature and studies (Shah et al. 2021). As shown in Fig. 9, the implementation of the copper electrodes in the reactor easily removed 48–58% of the xanthate even though the lowest level of electrical current was applied. Since the higher energy made more copper dissolve into the solution from the solid electrodes, this precipitating and coagulating agent in this system became more concentrated. As a result, much better results were obtained when the current increased up to 0.6 A, according to Model-3. As discussed in the previous cases, the solution pH was also critical for the electrocoagulation with the copper electrodes. When NaOH was incrementally added into the solution, a progressive improvement for the process was

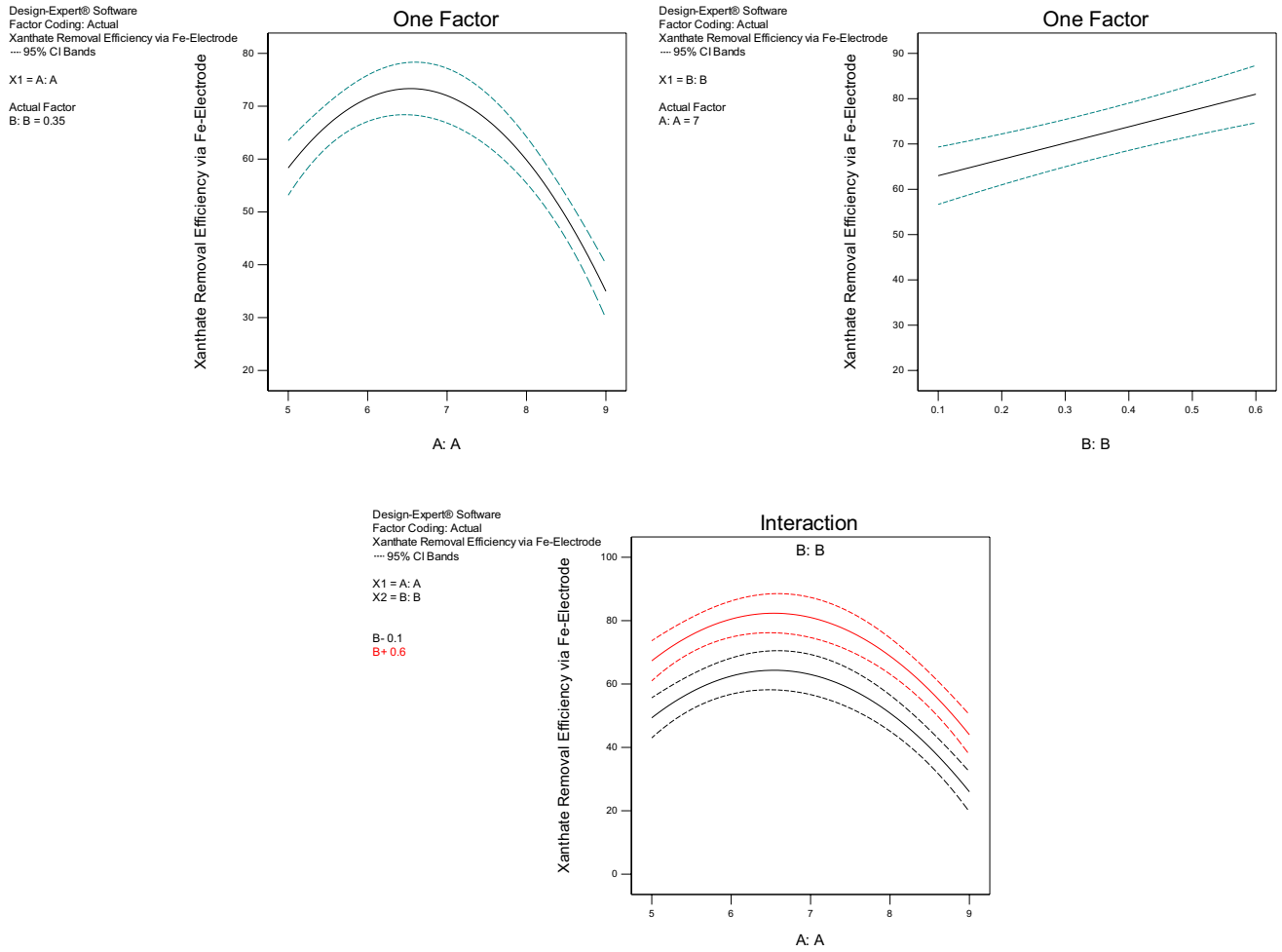

Fig. 8 Effect of individual factors and their synergistic interaction effect on xanthate removal when iron electrodes were implemented (Model-2)

observed. The best results (Fig. 9) were experienced at pH 9, reaching an almost complete xanthate removal level.

The aqueous chemistry of the copper–xanthate–water system contributes to the comprehension of the process. The interaction of aqueous copper and xanthate resulted in varying complexes in the form of cuprous and cupric species. These complexations were substantiated through several paths as a function of pH. Between pH 6 and 9, monovalent copper can form Cu(I) ethyl xanthate species in water.

$$Cu^{+} + X^{-} \rightarrow CuX \tag{1}$$

Another chemical reaction path reported in the literature (Voigt et al. 1994) was about the divalent copper. The hydroxyl species of Cu(II) can react with aqueous xanthate, and as a result, they form dixantogen, Cu(I) ethyl xanthate and Cu(II) ethyl xanthate (Scendo 2005). These reactions (2, 3) are not restricted to acidic and neutral pH levels (Voigt et al. 1994) in contradiction to the previously mentioned aqueous systems of iron and xanthate. When pH increased up to 9 as in this study, the reactions (2, 3) became more dominant. In this case, the performance of the process was mainly governed by the given reactions as follows.

$$Cu^{++} + 2X^{-} \rightarrow CuX + 1/2X_2 \tag{2}$$

$$4Cu^{++} + 8X^{-} \rightarrow 2CuX_2 + 2CuX + 1/2X_2 \tag{3}$$

The results of the experiments showed good parallelism with this specific literature information, and the performance of xanthate removal substantially improved up to ~ 100% by increasing pH to 9 thanks to the formation of both cupric xanthate and cuprous xanthate (Chang et al. 2002).

It should be noted that, in the scope of this work, all experiments were carried out with the clean electrodes, and also, the duration of the electrocoagulation process was limited. However, there can be a high tendency for the surface precipitation of cupric xanthate and/or cuprous xanthate (Souto et al. 1996) on the copper electrodes. If the above

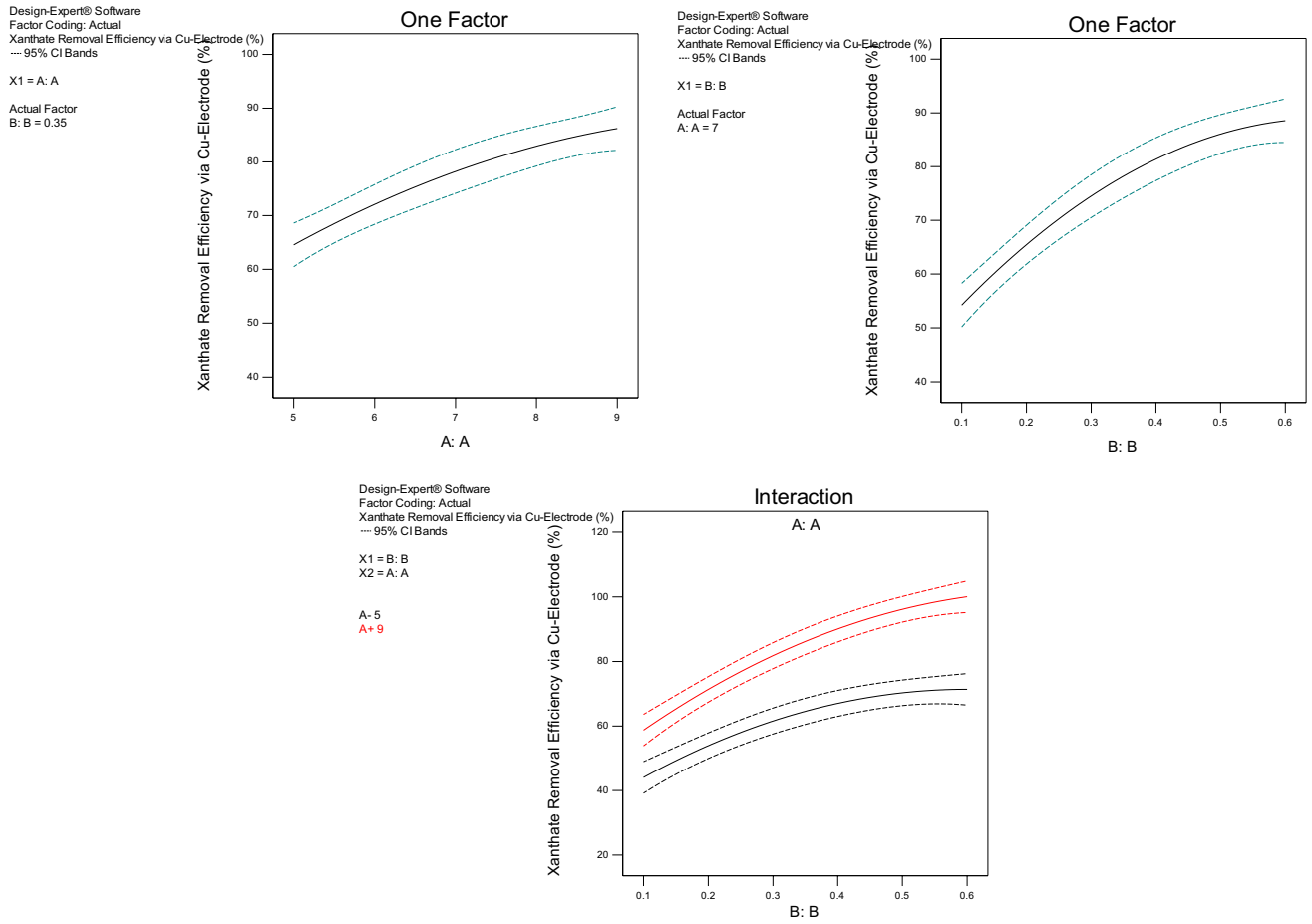

Fig. 9 Effect of individual factors and their synergistic interaction effect on xanthate removal when iron electrodes were implemented (Model-3)

precipitation reactions take place on the electrodes, the thin film growth of copper xanthate (Scendo 2005) can prevent the dissolution of copper ions from the electrodes, affecting the efficiency. Although the surface coverage of the electrodes always generates technical difficulties in any electrocoagulation process, the high affinity between the copper electrode and xanthate ions should be specifically considered for further similar researches.

After the effect of the parameters on the response was determined for each experimental setup and the related statistical model, the maximum removal percentages obtained with aluminum, iron and copper electrodes were determined at this stage of the work. The desirability studies were carried out for this purpose. The desirability contours were generated between 0 and 1 based on the response surfaces (Fig. 10) constructed on the previously estimated statistical equations (Table 4). In this contour map, 0 refers to non-desirable conditions, and 1 indicates the maximum desirability depending on the declared case-specific target (Maximization or Minimization of Removal Percentages) given in Table 5. When the minimization was targeted for the response variable, the aluminum, iron and copper electrodes could only remove 0%, 26.00% and 45.00% of the total aqueous xanthate. The main reasons for these low-efficient treatments were linked to the low electrical current application at 0.1 A and inappropriate aqueous chemistry, including the solution pH and the type of the hydrolyzable cation dissolved from the electrode.

On the other hand, to find out the most efficient process conditions for the highest removal percentages, the response variable was explicitly targeted to 100% (Desirability = 1) for each model, as stated in Table 5. The lowest desirability of 0.037 was estimated for this target when aluminum electrodes were used in the experiments. This value was very close to non-desirable zero, and it proved that aluminum electrodes yielded a result far from being acceptable with a removal% of only 3.67. The next maximum desirability was determined as 0.77 for Model-2: Electrocoagulation with iron electrodes (Table 4). The attachment of iron electrodes to the electrocoagulation reactor significantly enhanced the xanthate removal performance up to 82.34%. The

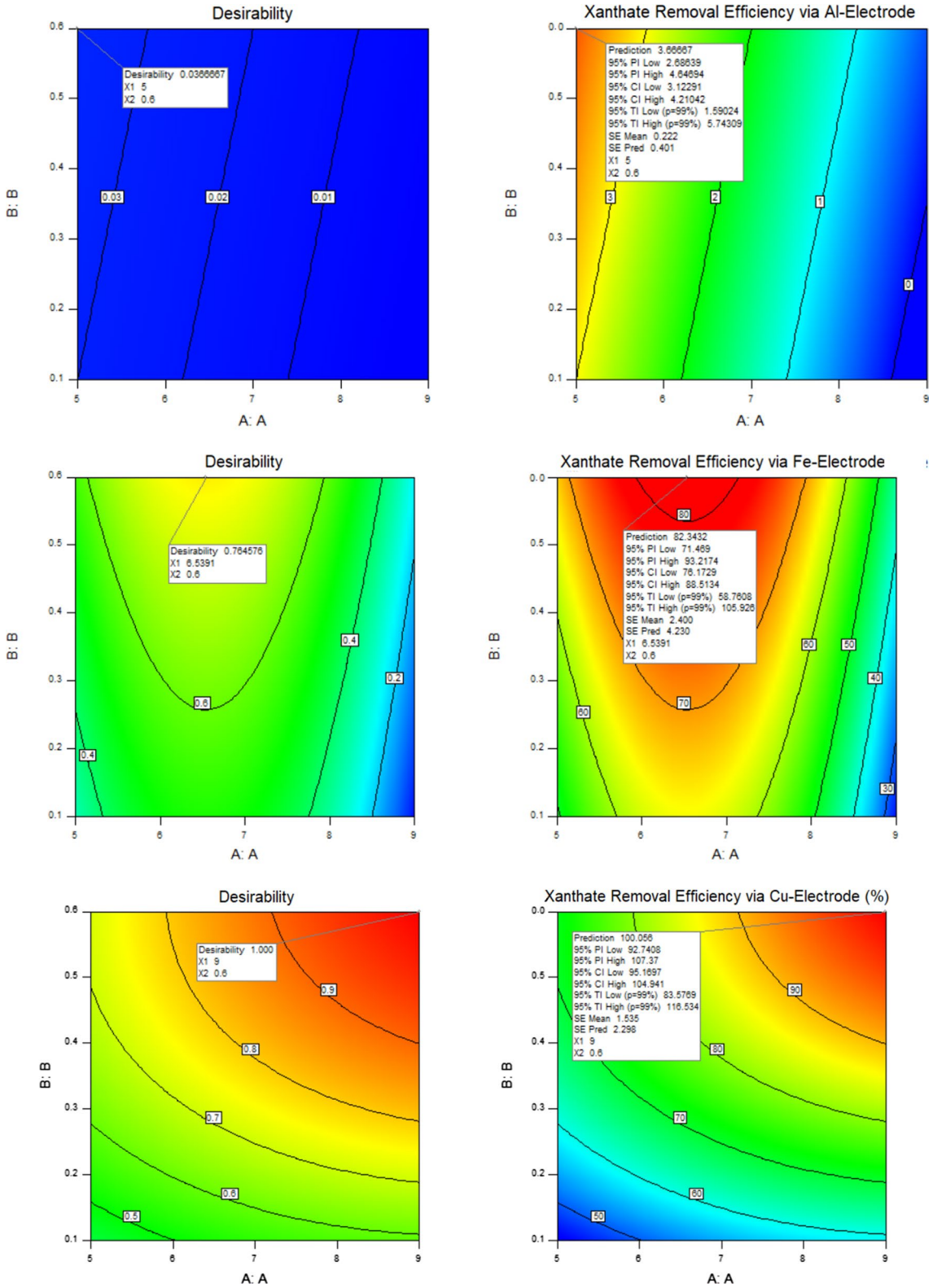

Fig. 10 Optimization work and the related response contours for the models (**a** Model-1 for aluminum electrode; **b** Model-2 for iron electrode; **c** Model-3 for copper electrode)

Table 4 Statistical models

Model-1: Electrocoagulation by using aluminum electrodes	Model-2: electrocoagulation by using iron electrodes	Model-3: Electrocoagulation by using copper electrodes
$Y=$	$Y=$	$Y=$
$+7.033$	-2210.10	$+18.140$
$-0.833*X_1$	$+82.833*X_1$	$+2.9667*X_1$
$+1.333*X_2$	$+36.00*X_2$	$+96.20000*X_2$
	$-6.333*X_1^2$	$+7.00000*X_1*X_2$
		$-109.333*X_1^2$

Y: Xanthate removal percentage/response variable

X_1: pH level

X_2: Applied electrical current

desirability work signified the solution pH at 6.54 and the electrical current at 0.60 A to reach this high removal rate. Notwithstanding the formation of hydroxyl ferric xanthates (Wang et al. 1989; Kydros et al. 1994) at these optimized values of the parameters, the aimed response percentages of 100% could not be achieved within the studied ranges. Nonetheless, the copper electrodes for the treatment were found very beneficial for the removal of xanthate. The desirability was estimated as 1 within a very narrow confidence of interval. Table 4 and Fig. 10 prove that a complete xanthate removal (100%) was succeeded by using copper electrodes instead of the iron and aluminum ones. The statistical optimization recommended the use of the highest level of pH (9) and the highest electrical current (0.59 A) for the efficacious electrocoagulation treatment. This statistical finding was tested three times in the laboratory, and the outcome, as shown in Fig. 11, checked the success of the water treatment under these optimized conditions. Xanthate was precipitated in the form of a yellow-colored solid matter (Fig. 12), and these residues sedimented very fast due to the optimized electrocoagulation process, leaving a clear supernatant.

In conclusion, the electrocoagulation method was qualified as a useful alternative technique for eliminating xanthate originated from mineral processing plants that focus on the concentration of complex sulfide ores. Furthermore, the performance tests based on the statistical methods proved that the aluminum electrodes used commonly for many other treatment purposes in the literature (Sillanpaa 2020) were not suitable for the removal of this harmful aqueous contaminant. Instead, the copper electrodes were designated the

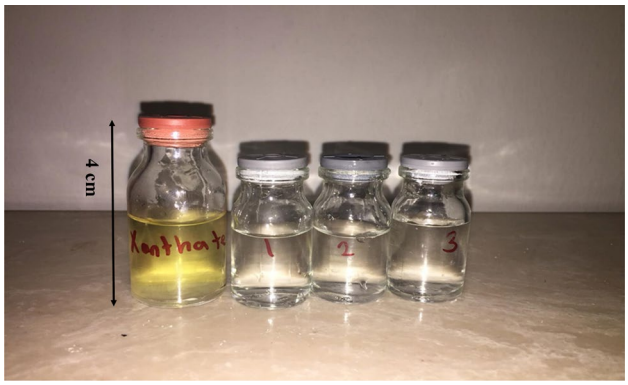

Fig. 11 Initial xanthate solution and the clean supernatants obtained with copper electrodes (pH 9 and 0.6 A and desirability = 1)

Table 5 Results of the optimization studies for varying target values

Model #	Case	Target	pH	Electrical current	Removal%	Lower bound of 95% confidence interval	Upper bound of 95% confidence interval	Desirability
Model 1 Electrocoagulation with Al electrodes	**Removal%** pH Electrical current	**Target → 100%** In range	5	0.6	3.67	3.12	4.21	0.037
	Removal% pH Electrical current	**Minimization** In range	8.95	0.12	0.00	−0.79	0.26	1.00
Model 2 Electrocoagulation with Fe electrodes	**Removal%** pH Electrical current	**Target → 100%** In range	6.54	0.60	82.34	76.17	93.22	0.77
	Removal% pH Electrical current	**Minimization** In range	9	0.1	26.00	19.67	32.33	1.00
Model 3 Electrocoagulation with Cu electrodes	**Removal%** pH Electrical current	**Target → 100%** In range	9.00	0.6	100.00	94.41	105.60	1.00
	Removal% pH Electrical current	**Minimization** In range	5.00	0.10	45.00	39.01	50.99	1.00

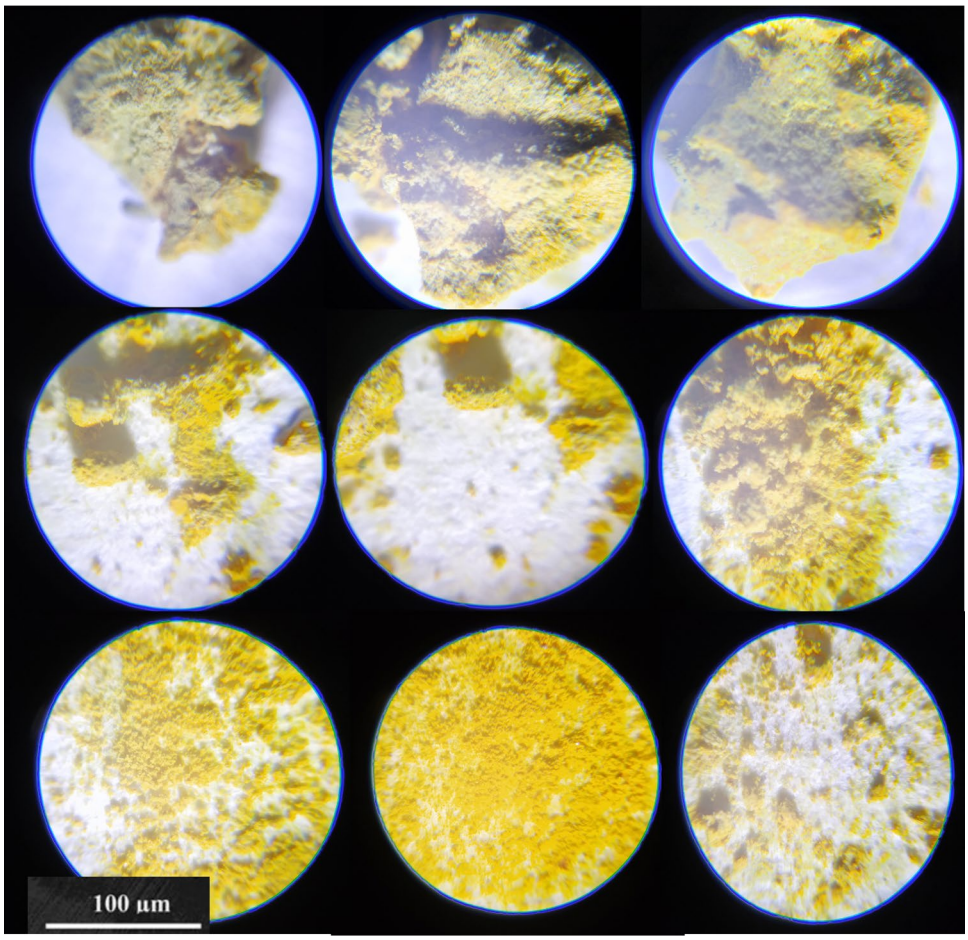

Fig. 12 Yellow-colored precipitates obtained with copper electrodes (pH 9 and 0.6 A and desirability = 1)

most effective ones for the electrocoagulation of xanthates among the followings:

$$\text{Removal\%}_{\text{Al electrodes}} < \text{Removal\%}_{\text{Fe electrodes}} < \text{Removal\%}_{\text{Cu electrodes}}$$

Conclusion

The mineral industry globally consumes a significant amount of xanthate to make sulfide particles' surface hydrophobic for the purpose of concentration. The discharged hazardous xanthate from the froth flotation plants contaminates the water bodies and causes health and safety issues, including infertility, toxicity, organ damage, corrosivity/irritation, etc. For this reason, in this study, the aqueous xanthate was aimed to be treated via electrocoagulation.

Three separate experimental setups were carried out with three different metal electrodes, namely aluminum, iron and copper, and three different statistical models were estimated via RSM. The most capable models were determined (all p-values for the models < 0.0015 and all adjusted R^2-values > 0.95) after the statistically nonsignificant terms were omitted from the mathematical models. Then, the performance evaluation and the optimization work were done by using response surfaces constructed based on the proposed linear and quadratic mathematical models (p-values of < 0.0001, 0.0011 and 0.0202, respectively).

The first model was about the effect of aluminum electrodes in the removal of xanthate. It was revealed that the increase in the solution pH from 5 to 9 generated a linear response surface indicating no change in the removal percentages. Similarly, the applied electrical current between 0.1 and 0.6 A did not succeed either. Aluminum ions released from the electrodes could not trigger the precipitation of xanthate during the electrocoagulation. The implementation of the aluminum electrodes was failed (Removal% = 3.67%) for this specific separation purpose since the maximum desirability was calculated as only 0.0037.

The second model showed a better performance for iron electrodes than the aluminum ones. 60% of the total xanthate was removed at 0.35 A when pH was 5. This removal % was

enhanced up to only 82.34% by adjusting the parameters. pH and electrical current were increased to 6.54 and 0.6 A, respectively, to reach this percentage (Desirability = 0.77). Nevertheless, the targeted desirability of 1 could not be met by this set of electrodes. On the other hand, at the alkaline pH, the performance of the process diminishes since the aqueous iron dissolved from the electrodes precipitated in the xanthate-free form. At pH 9, the yellow-colored water could not be cleared sufficiently due to the lack of stable hydroxyl ferric xanthates $Fe(OH)_2(EX)_{(solid)}$.

Thirdly, an uncommon copper electrode for the electrocoagulation was tested. Copper ions had a great affinity for xanthate molecules, and they formed Cu(I) ethyl xanthate and Cu(II) ethyl xanthate precipitates during the electrocoagulation. The related response surfaces showed that both input parameters contributed to the precipitation and sedimentation process. Whereas the lowest pH and electrical current levels produced the removal percent of 45%, the highest levels of these parameters managed to remove 100% of aqueous xanthate (Desirability = 1). Following the treatment, a very clear supernatant was obtained with a fast-sedimenting yellow-colored residue since copper ions have a strong complexation ability with xanthate. Consecutively, this combined statistical and experimental work manifested that the separation of hazardous xanthate from the water was possible using the electrocoagulation cell attached with copper electrodes. As a result, a superior removal of xanthate can be achieved with only copper electrodes rather than aluminum and iron.

Supplementary Information The online version contains supplementary material available at https://doi.org/10.1007/s11696-022-02120-4.

References

Ackerman PK, Harris GH, Klimpel RR, Aplan FF (1987) Evaluation of flotation collectors for copper sulfides and pyrite, I. Common sulfhydryl collectors. Int J Miner Process 21(1–2):105–127

Agorhom EA, Skinner W, Zanin M (2014) Diethylenetriamine depression of Cu-activated pyrite hydrophobised by xanthate. Miner Eng 57:36–42

Aitbara A, Cherifi M, Hazourli S, Leclerc JP (2016) Continuous treatment of industrial dairy effluent by electrocoagulation using aluminum electrodes. Desalin Water Treat 57(8):3395–3404

Akansha J, Nidheesh PV, Gopinath A, Anupama KV, Kumar MS (2020) Treatment of dairy industry wastewater by combined aerated electrocoagulation and phytoremediation process. Chemosphere 253:126652

Amin MI, Gado HS, Youssef WM, Masoud AM (2019) Precipitation of iron from wet process phosphoric acid using oxalic acid and potassium hexyl xanthate (PHX). Chem Pap 73(8):1871–1877

Amrollahi A, Massinaei M, Moghaddam AZ (2019) Removal of the residual xanthate from flotation plant tailings using bentonite modified by magnetic nano-particles. Miner Eng 134:142–155

Balouchi H, Baziar M, Dehghan A, Alidadi H, Shams M (2020) Combination of electrocoagulation and MOF adsorption systems for EBT removal from water. Int J Environ Anal Chem. https://doi.org/10.1080/03067319.2020.1737035

Bertillas U, Björklund I, Borg H, Hörnström E (1985) Biologiska effekter av xantater. Naturvårdsverket rapport 3112

Bertsch PM, Parker DR (1996) Aqueous polynuclear aluminum species. Environ Chem Alum 2:117–168

Bhattacharya S (2021) Central composite design for response surface methodology and its application in pharmacy. In: Response surface methodology in engineering science. IntechOpen

Boening DW (1998) Aquatic toxicology and environmental fate of xanthates. Miner Eng 50:65–68

Bowden JL, Young CA (2016) Xanthate chemisorption at copper and chalcopyrite surfaces. J S Afr Inst Min Metall 116(6):503–508

Bu X, Chen F, Chen W, Ding Y (2019) The effect of whey protein on the surface property of the copper-activated marmatite in xanthate flotation system. Appl Surf Sci 479:303–310

Chang YK, Chang JE, Lin TT, Hsu YM (2002) Integrated copper-containing wastewater treatment using xanthate process. J Hazard Mater 94(1):89–99

Chen Y, Liu X, Chen J (2021) Steric hindrance effect on adsorption of xanthate on sphalerite surface: a DFT study. Miner Eng 165:106834

DeMartino AW, Zigler DF, Fukuto JM, Ford PC (2017) Carbon disulfide: Just toxic or also bioregulatory and/or therapeutic? Chem Soc Rev 46(1):21–39

Deng Z, Cheng W, Tang Y, Tong X, Liu Z (2021) Adsorption mechanism of copper xanthate on pyrite surfaces. Physicochem Probl Miner Process 57:46–60

Farrokhpay S (2011) The significance of froth stability in mineral flotation: a review. Adv Colloid Interface Sci 166(1–2):1–7

Fornasiero D, Montalti M, Ralston J (1995) Kinetics of adsorption of ethyl xanthate on pyrrhotite: in situ UV and infrared spectroscopic studies. J Colloid Interface Sci 172(2):467–478. https://doi.org/10.1006/jcis.1995.1277

Grano SR, Prestidge CA, Ralston J (1997) Solution interaction of ethyl xanthate and sulphite and its effect on galena flotation and xanthate adsorption. Int J Miner Process 52(2–3):161–186. https://doi.org/10.1016/s0301-7516(97)00066-5

Hao F, Davey KJ, Bruckard WJ, Woodcock JT (2008) Online analysis for xanthate in laboratory flotation pulps with a UV monitor. Int J Miner Process 89(1–4):71–75. https://doi.org/10.1016/j.minpro.2008.07.004

Harjanto S, Haryono D, Nugraha H, Saputra G, Baidillah MR, Al Huda M, Taruno WP (2021) Gas holdup and bubble flow transition characteristics in column flotation process determined by capacitive signals measurement. Braz J Chem Eng 38:361–372

Hu C, Wang S, Sun J, Liu H, Qu J (2016) An effective method for improving electrocoagulation process: optimization of Al13 polymer formation. Colloids Surf A Physicochem Eng Asp 489:234–240

Kang W, Hu J (2017) Influence of the carbon atom numbers and the structure of collectors on the coal fines flotation. Cogent Eng 4(1):1323374

Karimifard S, Moghaddam MRA (2018) Application of response surface methodology in physicochemical removal of dyes from wastewater: a critical review. Sci Total Environ 640:772–797

Kydros KA, Gallios GP, Matis KA (1994) Electrolytic flotation of pyrite. J Chem Technol Biotechnol Int Res Process Environ Clean Technol 59(3):223–232

Mu Y, Peng Y, Lauten RA (2015) Electrochemistry aspects of pyrite in the presence of potassium amyl xanthate and a lignosulfonate-based biopolymer depressant. Electrochim Acta 174:133–142

Nasseri S, Yaqubov A, Alemi A, Nuriev A (2020) Optimization of copper and zinc ions removal from aqueous solution by modified

nano-bentonite using response surface methodology. J Ultrafine Grained Nanostruct Mater 53(1):78–90
Noirant G, Benzaazoua M, Kongolo M, Bussière B, Frenette K (2019) Alternatives to xanthate collectors for the desulphurization of ores and tailings: pyrite surface chemistry. Colloids Surf A Physicochem Eng Asp 577:333–346
Nyangi MJ (2021) Remediation of arsenic from water using iron and aluminum electrodes in electrocoagulation technology: adsorption isotherm and kinetic studies. Chem Afr 4(4):943–954
Palacios RJS, Kim DG, Ko SO (2016) Humic acid removal by electrocoagulation: characterization of aluminum species and humic acid. Desalin Water Treat 57(24):10969–10979
Prestidge CA, Thiel AG, Ralston J, Smart RSC (1994) The interaction of ethyl xanthate with copper(II)-activated zinc sulphide: Kinetic effects. Colloids Surf A Physicochem Eng Asp 85(1):51–68. https://doi.org/10.1016/0927-7757(94)02748-x
Rezaei R, Massinaei M, Moghaddam AZ (2018) Removal of the residual xanthate from flotation plant tailings using modified bentonite. Miner Eng 119:1–10
Saber WI, El-Naggar NEA, El-Hersh MS, El-Khateeb AY, Elsayed A, Eldadamony NM, Ghoniem AA (2021) Rotatable central composite design versus artificial neural network for modeling biosorption of Cr 6+ by the immobilized Pseudomonas alcaliphila NEWG-2. Sci Rep 11(1):1–15
Safwat SM, Hamed A, Rozaik E (2019) Electrocoagulation/electroflotation of real printing wastewater using copper electrodes: a comparative study with aluminum electrodes. Sep Sci Technol 54(1):183–194
Salarirada MM, Behnamfardb A, Veglioc F (2021) Removal of xanthate from aqueous solutions by adsorption onto untreated and acid/base treated activated carbons. Desalin Water Treat 212:220–233
Scendo M (2005) Potassium ethyl xanthate as corrosion inhibitor for copper in acidic chloride solutions. Corros Sci 47(7):1738–1749
Shah M, Sarkar A, Mandal S (2021) Wastewater treatment. Elsevier Gezondheidszorg
Sharma K, Goswami M, Shadab M, Sarma NS, Devi A (2021) Treatment of paper mill effluent via electrochemical reaction and assessment of antibacterial activity of ZnO nanoparticles in in-vitro conditions. Chem Pap 75:3921–3929
Sheikh N, Leja J (1977) Msssbauer Spectroscopy of Fe-Xanthates Sep Sci 12(5):529–540
Sheikh N (1972) The chemical stability of the heavy metal xanthates. Ph.D. thesis, University of British Columbia, Canada
Shen Y, Nagaraj DR, Farinato R, Somasundaran P (2016) Study of xanthate decomposition in aqueous solutions. Miner Eng 93:10–15
Shen Y, Zhou P, Zhao S, Li A, Chen Y, Bai J, Han C, Wei D, Ao Y (2020) Synthesis of high-efficient TiO_2/clinoptilolite photocatalyst for complete degradation of xanthate. Miner Eng 159:106640
Sillanpaa M (2020) Advanced water treatment: electrochemical methods, 1st edn. Elsevier, Amsterdam
Souto RM, Fox V, Laz MM, Perez M, González S (1996) Some experiments regarding the corrosion inhibition of copper by benzotriazole and potassium ethyl xanthate. J Electroanal Chem 411(1–2):161–165
Sun Z, Forsling W (1997) The degradation kinetics of ethyl-xanthate as a function of pH in aqueous solution. Miner Eng 10(4):389–400. https://doi.org/10.1016/s0892-6875(97)00016-2
Sürme Y, Demirci OB (2014) Determination of direct violet 51 dye in water based on its decolorisation by electrochemical treatment. Chem Pap 68(11):1491–1497
Voigt S, Szargan R, Suoninen E (1994) Interaction of copper (II) ions with pyrite and its influence on ethyl xanthate adsorption. Surf Interface Analy 21(8):526–536
Vučinić DR, Lazić PM, Rosić AA (2006) Ethyl xanthate adsorption and adsorption kinetics on lead-modified galena and sphalerite under flotation conditions. Colloids Surf A Physicochem Eng Asp 279(1–3):96–104
Wang X, Eric Forssberg KS, Bolin NJ (1989) Thermodynamic calculations on iron-containing sulphide mineral flotation systems, I. The stability of iron-xanthates. Int J Miner Process 27(1–2):1–19. https://doi.org/10.1016/0301-7516(89)90002-1
Wang H, Wen S, Han G, Feng Q (2019) Effect of copper ions on surface properties of $ZnSO_4$-depressed sphalerite and its response to flotation. Sep Purif Technol 228:115756
Xia L, Hart B, Larachi F, Gravel O (2019) Galvanic interaction of pyrite with Cu activated sphalerite and its effect on xanthate adsorption. Can J Chem Eng 97(10):2671–2677
Xu Y, Lay JP, Korte F (1988) Fate and effects of xanthates in laboratory freshwater systems. Bull Environ Contam Toxicol 41(5):683–689
Zini LP, Longhi M, Jonko E, Giovanela M (2020) Treatment of automotive industry wastewater by electrocoagulation using commercial aluminum electrodes. Process Saf Environ Prot 142:272–284